Biochimica et Biophysica Acta, 1108 (1992) 91–98

BBAMEM 75684

Triiodothyronine binding sites in the rat erythrocyte membrane: involvement in triiodothyronine transport and relation to the tryptophan transport System T

Michel Samson, Jeannine Osty, Jacques Francon and Jean-Paul Blondeau

Unité de Recherche sur la Glande Thyroïde et la Régulation Hormonale (U.96), Institut National de la Santé et de la Recherche Médicale, Le Kremlin-Bicêtre, (France)

(Received 6 April 1992)

Key words: Thyroid hormone; Tryptophan; Triiodothyronine-binding site; Amino acid transport; Erythrocyte membrane

The binding of L-triiodothyronine (T_3) to rat erythrocyte membranes (ghosts and peripheral protein-depleted vesicles) was studied under equilibrium conditions. Ghosts contained high-affinity T_3-binding sites whose dissociation constant (21 nM) was similar to the equilibrium-exchange Michaelis constant of T_3 transport measured in ghosts. Each ghost contained about $8 \cdot 10^3$ high-affinity binding sites. The high affinity T_3 binding was stereospecific and was inhibited by L-tryptophan (Trp) but not by L-leucine. The iodothyronine and amino acid specificity of binding is therefore similar to that of System T, the erythrocyte T_3/Trp transporter. These Trp-inhibitable high-affinity T_3-binding sites were also present in peripheral protein-depleted membrane vesicles, indicating that they are integral part of the membrane. Ghosts prepared from human erythrocytes, which have very low System T transport activities, contained no detectable Trp-inhibitable high-affinity T_3-binding sites. In rat erythrocyte ghosts, *N*-ethylmaleimide inactivated both the binding and the transport of T_3. This inactivation was blocked by T_3 and Trp with similar efficiencies. Phenylglyoxal, an arginine residue modifier, also inhibited both high-affinity T_3 binding and System T transport activity. It is concluded that the Trp-inhibitable high-affinity T_3-binding sites in the rat erythrocyte membrane are likely to be associated with System T.

Introduction

The thyroid hormones, 3,5,3'-triiodo-L-thyronine (T_3) and thyroxine (T_4), must cross the plasma membrane of target cells to reach the deiodinase enzymes and the T_3 nuclear receptors before they can express their biological activity. They are carried across the membrane by saturable, stereospecific transport systems which facilitate thyroid hormone uptake and/or concentrate the hormones intracellularly [1–5].

The mature mammalian erythrocytes are not considered to be target cells for thyroid hormones because they have no nucleus. However, T_3 is transported across the plasma membrane of rat erythrocytes by a stereospecific, Na^+-independent carrier [6,7]. The carrier in rat erythrocytes is 500-times more active than that in human erythrocytes [8]. T_4 inhibits T_3 transport, but is not itself transported across the plasma membranes of rat or human erythrocytes [6,8].

Erythrocytes also possess an intracellular trapping system for thyroid hormones which may, in part, involve T_3 binding to cytosol proteins [6,8]. As a result of this intracellular binding activity, erythrocytes accumulate T_3 (50 times over the free extracellular concentration) and erythrocyte-associated T_3 represents about 25% of the total plasma T_3 (free + plasma protein-bound). It has therefore been suggested that the rat erythrocytes are involved in blood transport and peripheral delivery of T_3 [9], with the membrane carrier allowing rapid equilibration ($t_{1/2} = 3$ s) of the erythrocyte-associated T_3 with the free circulating compartment.

We have also shown [10] that the T_3 transport system of rat erythrocytes is closely related to System T, the aromatic amino acid carrier originally found in human erythrocytes [11,12]. The kinetics of transport are compatible with a common simple carrier of T_3 and L-tryptophan (Trp) or a set of interactive transport systems, which can perform countertransport of T_3 and aromatic amino acids [13].

T_3-binding sites have been reported in the membranes of a variety of cell types [14–16], including erythrocytes [17]. However, the function of these sites is still unclear: whether they take part in the transport of thyroid hormones across the plasma membrane, or

Correspondence to: J.P. Blondeau, U.96 INSERM, 80 rue du Général Leclerc, 94276 Kremlin-Bicêtre, France.

Abbreviations: BSA, bovine serum albumin; NEM, *N*-ethylmaleimide; T_4, thyroxine; T_3, 3,5,3'-triiodo-L-thyronine; D-T_3, 3,5,3'-triiodo-D-thyronine; Trp, L-tryptophan.

they are receptors involved in nongenomic effects of these hormones [18,19].

The first part of this study was conducted to define the conditions for measuring T_3 binding to rat erythrocyte membranes (ghosts and peripheral protein-depleted vesicles). These methods were then used to show that these membranes contain high-affinity T_3-binding sites related to System T. This was done by correlating T_3-binding properties, measured under equilibrium conditions, with T_3 transport kinetics, measured under initial velocity conditions, using the criteria of: saturability, substrate specificity, species specificity and irreversible inhibition by amino acid reagents. Part of this work has been reported in abstract form [20].

Experimental procedures

Erythrocyte ghosts and membrane vesicles. Male Wistar rats (200 g body weight, Iffa Credo, France) were killed by decapitation. Blood was collected over heparin; erythrocytes were separated by centrifugation and washed as previously described [6]. Erythrocyte ghosts were prepared, according to Steck and Kant [21], by osmotic lysis in 30 vols. of buffer A (5 mM sodium phosphate buffer (pH 8.0), containing 0.3 mM phenylmethylsulfonyl fluoride) and centrifugation at 22500 × *g* for 15 min. White ghosts were obtained by washing the membrane pellet three times with 30 vols. of buffer A; they were resealed by incubation (40 min at 37°C) in buffer B (125 mM NaCl, 20 mM KCl, 4 mM $MgCl_2$, 10 mM glucose, 4.05 mM Na_2HPO_4, 0.95 mM NaH_2PO_4 (pH 7.4)). Peripheral-protein-depleted membrane vesicles were prepared according to Jarvis and Young [22], by homogenizing unsealed ghosts (3 mg protein/ml) in 6 vols. of solution C (0.1 mM EDTA, 0.3 mM phenylmethylsulfonyl fluoride (pH 11.2)) for 15 min at 0°C, centrifuging them (100000 × *g*, 30 min) and washing with buffer B. Polyacrylamide gel electrophoresis in sodium dodecyl sulphate (not shown) indicated that the vesicles were almost completely depleted of peripheral skeletal proteins, except for some residual band 4.2. Assay of NADH–cytochrome-*c* oxydoreductase in the presence and absence of saponin [21] indicated that the vesicles were approx. 95% inside out (not shown). Human blood was obtained from volunteers (40–50-year old) and human erythrocyte ghosts were prepared as described above. Cell and ghost concentrations were determined in a Coulter counter. Protein was assayed by the Lowry procedure.

Measurement of membrane-associated T_3 and Trp. Stop/wash procedure [7,10]: membranes were incubated with [^{125}I]T_3 or [^{3}H]Trp and the incubation was stopped with an ice-cold solution of unlabelled T_3 (10 μM final concentration) in buffer B. The membranes were centrifuged (15000 × *g*, 4 min) and washed twice with buffer D (137 mM NaCl, 2.7 mM KCl, 8.1 mM Na_2HPO_4. 1.5 mM KH_2PO_4 (pH 7.5)) containing 10 μM unlabelled T_3. Radioactivity was measured on the washed pellets.

Dowex resin adsorption method [23]: membranes were incubated with [^{125}I]T_3 and then treated with 1/10 vol. of a Dowex suspension (600 mg/ml in buffer B). The mixture was shaken for 2 min at 0°C, centrifuged (55 × *g*, 1 min) and aliquots of the supernatant were immediately taken for determination of bound radioactivity.

Measurement of T_3 and Trp transport by ghosts. Transport experiments were performed at 25°C. Zero-*trans* uptake of T_3 was initiated by mixing ghosts with buffer B containing [^{125}I]T_3 (10^5 cpm/ml), and various additives, to obtain a final suspension containing $4 \cdot 10^8$ ghosts/ml. Zero-*trans* uptake of Trp was performed similarly, except that the mixture contained [^{3}H]Trp ($8 \cdot 10^5$ cpm/ml) and $2 \cdot 10^9$ ghosts/ml. For equilibrium-exchange uptake, ghosts were preloaded with various concentrations of unlabelled T_3 until equilibrium was reached (60 min at 25°C). The ghosts were centrifuged at 25°C and [^{125}I]T_3 (10^5 cpm/ml) was added to the supernatants in a negligible (1%) volume before reconstitution with the ghost pellets. The equilibrium concentration of T_3 was determined in parallel incubations performed in the presence of an additional trace amount of labelled T_3, as described in Ref. 7, assuming equal intra- and extra-cellular concentrations of free T_3 at equilibrium. Transport was terminated by the stop/wash procedure and the radioactivity of the ghost pellets was determined in a γ-counter, for [^{125}I]T_3, or by liquid scintillation, after solubilization and deproteinization, for [^{3}H]Trp [10]. Initial velocity conditions were as follows: the zero-time values were subtracted from those obtained after 3 s at 25°C. All assays were performed in duplicate.

Efflux and dissociation experiments. Ghosts ($4.6 \cdot 10^8$ ghosts/ml) or depleted vesicles (0.15 mg of protein/ml) were incubated at 0°C with [^{125}I]T_3 (10^5 cpm/ml) until equilibrium was reached. Dissociation was induced: (1) by isotopic dilution (adding 1 μM unlabelled T_3 in a negligible volume) followed, after various times at 0°C, by a 2-min treatment with Dowex resin, (2) by contact with Dowex resin for various times at 0°C, with a minimum of 2 min (taken as time zero of dissociation to allow comparison with the isotopic dilution procedure).

Equilibrium binding assays. $4 \cdot 10^8$ ghosts/ml were incubated with [^{125}I]T_3 (10^5 cpm/ml) and additives in buffer B for 60 min at 25°C (rat erythrocyte ghosts), or for 40 min at 37°C (human erythrocyte ghosts), to reach equilibrium. Ghost-associated T_3 was determined by the stop/wash procedure. Unbound T_3 was calculated by subtracting bound from total T_3.

Vesicles (0.1 mg protein/ml in buffer B) were incu-

bated with [^{125}I]T_3 (10^5 cpm/ml) for 10 min at 25°C and centrifuged at 9400 × *g* for 15 min at 25°C, without perturbing equilibrium (centrifugation procedure). Aliquots of the supernatants were counted for radioactivity and bound T_3 was calculated by difference with total T_3.

N-Ethylmaleimide (NEM) inhibition. Washed erythrocytes ($4.5 \cdot 10^7$ cells/ml) were preincubated in buffer B with or without unlabelled T_3 (10 μM) or Trp (10 mM) and, 15 min later, with or without NEM (1 mM) for 60 min at 25°C. The incubations were stopped by adding a chilled solution of mercaptoethanol (final concentration: 3 mM). The cells were centrifuged, washed once with buffer B, suspended in buffer B containing 1.5% bovine serum albumin (BSA), and incubated for 20 min at 37°C. This procedure was repeated once to remove all unlabelled T_3 or Trp. The erythrocytes were then washed twice in buffer B, ghosts were prepared as described above, and binding assays and uptake experiments were performed.

Phenylglyoxal inhibition. Erythrocytes ($1.5 \cdot 10^8$ cells/ml) were incubated with or without phenylglyoxal (final concentration: 10 mM) at 37°C. The incubations were stopped by adding chilled buffer B. The cells were centrifuged immediately, washed with cold buffer B containing 0.5% BSA and resuspended in buffer B-BSA. Irreversible binding of phenylglyoxal was obtained after a 20-h incubation at 0°C [24]. The erythrocytes were then washed twice in buffer B and used either to prepare ghosts, or to measure initial influx velocities as described in [10], except that the cell concentrations were $1.5 \cdot 10^8$ cells/ml for [^{125}I]T_3 uptake and $6 \cdot 10^8$ cells/ml for [^{3}H]Trp uptake.

Statistical treatment of data. Standard deviations were calculated according to Snedecor and Cochran [25]. The values of dissociation constants (K_d), maximal binding capacities (B_{max}) and inhibition constants (K_i) were obtained by nonlinear least-square curve fitting, using an adaptation (Biosoft, UK) for the Apple-Macintosh of the Ligand program of Munson and Rodbard [26]. This program performs statistical analysis (*F*-test) of the reduction in the residual variance given the change in the model (e.g., one-site vs. two-site).

Materials. L-[3′-^{125}I]T_3 (spec. act. 3 mCi/μg) and L-[5-^{3}H]Trp (spec. act. 30 Ci/mmol) were from Amersham (UK). Unlabelled T_3, T_4, 3,5,3′-triiodo-D-thyronine (D-T_3), L-amino acids, BSA (fraction V), NEM, phenylglyoxal and phenylmethylsulfonyl fluoride were from Sigma. The Dowex AG 1-X8 resin was from Bio-Rad. All other chemicals were of analytical grade. Plastic tubes and pipette tips were siliconized (Sigmacote, Sigma).

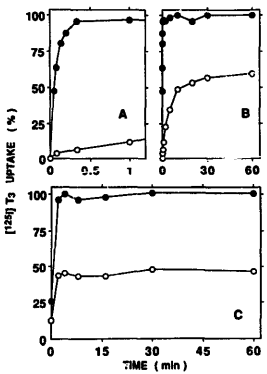

Fig. 1. Time-course of T_3 uptake by rat erythrocyte ghosts and depleted vesicles. Rat erythrocyte ghosts were incubated at 25°C (panels A and B), and depleted vesicles were incubated at 0°C (panel C), in the presence of 0.2 nM [^{125}I]T_3 with (○) or without (●) excess unlabelled T_3 (10 μM, panels A and B or 1 μM, panel C). At timed intervals, ghost-associated T_3 was determined by the stop/wash procedure and vesicle-associated T_3 was determined by the Dowex adsorption method, as described under Experimental procedures. Results (means of duplicates) are expressed as the percentage of the 10-min uptake value (20 fmol/10^8 ghosts, panels A and B) or of the 4-min uptake value (7.6 fmol/100 μg of protein, panel C), measured in the absence of unlabelled T_3. The time scales are 0–1 min (A) or 0–60 min (B and C).

Results and Discussion

1. Uptake and binding of T_3 by ghosts and inside-out vesicles

Figs. 1A and 1B show the time-course of T_3 uptake by ghosts at 25°C by the stop/wash procedure. Uptake of a tracer amount (0.2 nM) of labelled T_3 reached equilibrium by 20 s (half-time ≈ 3 s, Fig. 1A), whereas at least 30 min were necessary (Fig. 1B) in the presence of excess unlabelled T_3 (10 μM, a concentration reported [6] to saturate the erythrocyte carrier). The initial velocity of uptake was almost completely inhibited (70-fold) in the presence of excess unlabelled T_3 (Fig. 1A), whereas the equilibrium level was partly saturable (40% lower in the presence of 10 μM T_3, Fig. 1B).

We previously reported that T_3 was apparently concentrated, at equilibrium, inside erythrocytes by intracellular trapping. This was due, in part, to T_3 binding by cytosol proteins [6]. The present experiments show that white ghosts also accumulate T_3, suggesting that membrane-associated proteins (and perhaps membrane lipids) participate in the intracellular binding.

Equilibrium uptake of 0.2 nM T_3 was reached in ghosts in about 30 min at 0°C, but at least 48 h were

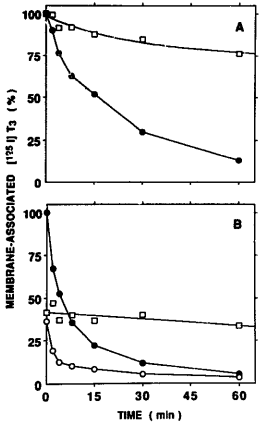

Fig. 2. Time-course of T_3 efflux and dissociation. Rat erythrocyte ghosts (panel A) were incubated for 60 min, and depleted vesicles (panel B) were incubated for 10 min, at 0°C, with [^{125}I]T_3 (0.2 nM) and with (○) or without (●, □) 1 μM unlabelled T_3, as described under Experimental procedures. Dissociation was followed either in the presence of Dowex in the medium (●, ○) or after isotopic dilution with 1 μM unlabelled T_3 (□), as described under Experimental procedures. Results (means of duplicates) are expressed as the percentage of the zero-time value (24.3 fmol/10^8 ghosts and 10.4 fmol/100 μg vesicle proteins).

necessary at 10 μM T_3 (not shown). This precluded saturation studies of the equilibrium binding level at 0°C. In contrast, T_3 uptake by inside-out vesicles depleted of extrinsic proteins could be followed at 0°C by the Dowex adsorption method (Fig. 1C). No saturable initial transport step was observed within the time resolution of the experiment, even at this low temperature. Equilibrium was reached within the first two min of incubation, both in the presence and absence of excess unlabelled T_3. Nevertheless, about 50% of the equilibrium T_3 binding appeared saturable.

2. *T_3 efflux and dissociation from ghosts and vesicles*

The time-course of T_3 release from ghosts and inside-out vesicles preloaded with labelled T_3 was studied at 0°C with Dowex in the medium. The half-time for dissociation from ghosts was about 15 min (Fig. 2A). In contrast, isotopic dilution induced no significant release of labelled T_3. This is because of the *trans*-inhibition of efflux, which has been kinetically characterized in intact erythrocytes [7], and indicates that there is a transport step before dissociation of T_3 from the membrane. Therefore, all the ghost-associated T_3 at equilibrium (saturable plus nonsaturable binding) was internalized.

Inside-out vesicles were preincubated with labelled T_3 (0.2 nM) in the presence or absence of excess unlabelled T_3 (1 μM), and dissociation was studied at 0°C with Dowex in the medium (at 25°C, dissociation was too rapid to be measurable by this method). The half-life of dissociation from 0.2 nM-preloaded vesicles was about 4 min (Fig. 2B). No saturation kinetics of efflux were observed since dissociation from 1 μM-preloaded vesicles proceeded with a half-life of about 2 min. Unlike the situation in ghosts, isotopic dilution induced an almost immediate dissociation of the saturable part of the binding. This precluded the use of the stop/wash procedure for measuring binding to vesicles.

When substrate binding occurs, uptake may or may not represent transport across the membrane, depending on the sidedness of the binding sites [27]. Taken together, our results suggest that the T_3-binding sites, including saturable binding sites, are located at the inner surface of the membrane in sealed white ghosts, and are on the outside of inside-out vesicles.

3. *Saturability of equilibrium T_3 binding*

The equilibrium binding of [^{125}I]T_3 to rat erythrocyte ghosts was studied after 60-min incubations at 25°C with increasing concentrations of unlabelled T_3 (25 pM–10 μM) in order to measure binding to the exclusion of transport. The binding isotherm was resolved into three components using the Ligand program: two classes of saturable binding sites plus a nonsaturable component. A plot of the Scatchard-transformed data, obtained after subtraction of the nonsaturable binding component, is shown in Fig. 3A. Lines representing binding of T_3 to each category of sites are also included. The inset shows the linear relationship obtained after subtraction of the contribution of the low-affinity binding component. The dissociation constant (K_d) of the high-affinity sites was 21 ± 4 nM and the maximal binding capacity (B_{max}) was 1.3 ± 0.2 pmol/10^8 ghosts (mean values ± S.D. of seven independent experiments). This B_{max} value corresponds to (8.0 ± 1.1) · 10^3 T_3-binding sites per ghost (mean ± S.D., n = 7). The apparent K_d of the low-affinity sites was approx. 50 μM and the B_{max} was approx. 4 nmol/10^8 ghosts.

The equilibrium-exchange transport of T_3 in ghosts, measured at 25°C under initial velocity conditions (as described under Experimental procedures), followed simple Michaelis kinetics (not shown). The kinetic parameters (mean of two independent experiments performed with different preparations of ghosts), calculated by linear regression from Eadie-Hofstee plots of the data (not shown) were K^{ee} = 18 (range: 16–21) nM

and $V^{cc} = 8.9$ (range: 8.4–9.4) pmol/min per 10^8 ghosts. The K^{cc} is similar to that reported previously [7] for transport in intact erythrocytes, but the maximal velocity is about 50% lower, suggesting some loss of transport activity during ghost preparation.

The K_d of the high-affinity sites is therefore in good agreement with the K^{cc} for equilibrium-exchange transport, as expected for binding to a conventional type (simple) carrier [28]. This suggests that the reported high-affinity T_3 binding at equilibrium is to the carrier itself.

The binding constants of depleted vesicles were also measured at 25°C by the centrifugation method (see Experimental procedures). Again, two classes of saturable binding sites plus a nonsaturable component were found (Fig. 3B). The K_d of the high-affinity sites was 15 nM (mean of two independent experiments, range: 14.5–15.5) and the B_{max} was 140 pmol/mg protein (range: 137–143). On the basis of the protein content of ghosts (approx. 33 μg/10^8 ghosts) the high-affinity T_3 binding sites were enriched approximately

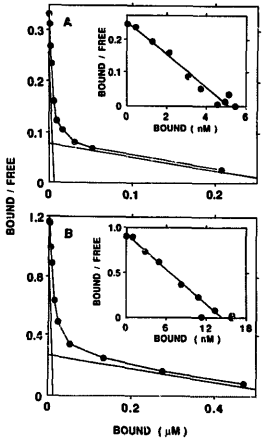

Fig. 3. Saturability of equilibrium T_3 binding. Equilibrium binding was measured in rat erythrocyte ghosts (panel A) or depleted vesicles (panel B) as described under Experimental procedures. Binding data (means of duplicates) were analysed by a computerized procedure (see Experimental procedures) and a Scatchard plot was constructed after subtraction of the non-saturable binding component (bound/free ratio = 0.25 for ghosts and 0.61 for vesicles). The straight lines represent the high- and low-affinity saturable binding components. Insets: plots of the Scatchard-transformed data obtained after subtraction of the low-affinity binding components.

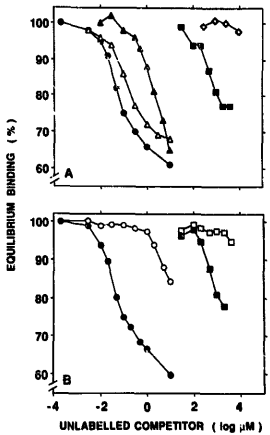

Fig. 4. Specificity of equilibrium T_3 binding in rat and human erythrocyte ghosts. Equilibrium [^{125}I]T_3 binding to rat erythrocyte ghosts (panel A) was measured in the presence of increasing concentrations of the following unlabelled competitors: T_3 (●), T_4 (△), D-T_3 (▲), Trp (■), leucine (◇), as described under Experimental procedures. Equilibrium [^{125}I]T_3 binding to human (○, □) and rat (●, ■) erythrocyte ghosts (panel B) was also measured in the presence of increasing concentrations of unlabelled T_3 (●, ○) or Trp (■, □). The results are the means of duplicates and are expressed as the percentage of the equilibrium binding measured in the absence of competitor (18, 16 and 13 fmol/10^8 ghosts, respectively, for rat membranes in panel A and for rat and human membranes in panel B).

4-fold by removal of extrinsic membrane proteins. Low-affinity sites (apparent $K_d \approx 3$ μM) were also present in vesicles, but their concentration ($B_{max} \approx 10$ nmol/mg protein) was about 10-times lower than in ghosts.

Botta et al. [17] reported the presence of a set of very high-affinity T_3 binding sites ($K_d \approx 10$ and 200 pM) in rat erythrocyte membrane vesicles depleted of peripheral membrane proteins. The very high affinity of these sites and the fact that they were dependent on heating and proteolysis [29] makes it unlikely that they are involved in T_3 transport. In our hands, T_3 concentrations as low as 25 pM provided no evidence that rat erythrocyte ghosts or inside-out vesicles possessed binding sites with such a high affinity.

4. Specificity of the high-affinity T_3 binding to rat erythrocyte membranes

Fig. 4A shows that the equilibrium binding of labelled T_3 was displaced by unlabelled iodothyronine

analogues and Trp in a concentration-dependent manner. The inhibition constants for the high-affinity binding sites (K_i), calculated by nonlinear curve fitting, were 72 ± 17 nM ($n = 3$) for unlabelled T_4 and 0.95 μM (range: 0.7–1.2 μM, $n = 2$) for unlabelled D-T_3. Trp inhibited the high-affinity T_3 binding with a K_i of 0.35 mM (range: 0.34–0.36 mM, $n = 2$) and was without effect on the low-affinity sites (best fit obtained with a one-site binding model plus nondisplaceable binding). Leucine (up to 10 mM) did not inhibit T_3 binding.

The rank order of analogue apparent affinity ($T_3 > T_4 >$ D-$T_3 >$ Trp ≫ leucine) is identical to that determined under initial velocity conditions in zero-*trans* influx experiments, performed either with intact erythrocytes [6,10] or with ghosts (present work, not shown). This indicates for a relationship between the high-affinity T_3-binding sites in erythrocyte membranes and the T_3/Trp transport system previously characterized in intact rat erythrocytes [10,13].

The ability of Trp to inhibit labelled T_3 binding was also studied in depleted vesicles, at 25°C, by the centrifugation method (not shown). Only the high-affinity T_3 binding was inhibited, with a K_i (calculated by nonlinear curve fitting) of 0.22 mM (mean of two independent experiments, range: 0.20–0.25). Leucine (up to 10 mM) was not inhibitory. These results confirm that the Trp-inhibitable high-affinity T_3-binding sites in membranes from rat erythrocytes are not borne by skeletal or other peripheral membrane proteins.

5. T_3 binding to human erythrocyte ghosts

The T_3/Trp transport activity of human erythrocytes is 350–500-times lower than that of rat erythrocytes [8,10]. Fig. 4B indicates that the equilibrium binding of [^{125}I]T_3 to human erythrocyte ghosts is not significantly displaced by unlabelled T_3 at concentrations from 0.2 nM to 1 μM, or by unlabelled Trp up to 2 mM. The competition curves obtained with rat erythrocyte ghosts are also plotted in Fig. 4B, for comparison, showing high-affinity T_3-binding sites and competition by Trp. Only low-affinity T_3-binding sites were detected in human erythrocyte ghosts, with $K_d > 25$ μM, similar to the low affinity sites detected in rat erythrocyte ghosts. Two independent experiments performed with erythrocytes from different donors gave the same results.

Therefore, the lack of detectable Trp-inhibitable high-affinity T_3-binding sites in the plasma membrane of human erythrocytes may be correlated with the very low activity of the T_3/Trp transport system in these cells.

6. Effect of NEM on T_3 binding

We previously reported that the T_3 and Trp transport systems in intact rat erythrocytes were irreversibly

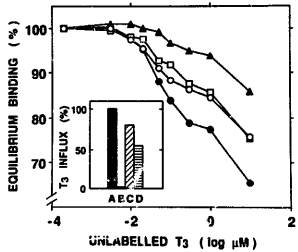

Fig. 5. Effect of NEM on T_3 equilibrium binding and T_3 influx. Rat erythrocytes were preincubated with buffer (●, ▲) or buffer containing 10 μM T_3 (○) or buffer containing 10 mM Trp (□) and further incubated in the absence (●) or presence (○, □, ▲) of 1 mM NEM, as described under Experimental procedures. Incubations were stopped, erythrocytes were washed (see Experimental procedures) and ghosts were prepared. Equilibrium T_3 binding was measured in ghosts and the results (mean of duplicates) were expressed as the percentage of the control value (15 fmol/10^8 ghosts) Inset: initial velocities of T_3 uptake were determined in ghosts and expressed as the percentage of the control value (80 fmol/min per 10^8 ghosts). Column A: control; column B: NEM-treated; column C: NEM-treated, T_3-protected; column D: NEM-treated, Trp-protected.

inhibited by NEM, and that each substrate protected the transport system of the other against inactivation [10]. We therefore studied the inhibition of L-T_3 binding to ghosts prepared from NEM-pretreated rat erythrocytes, and the protection of the binding sites by T_3 and Trp (Fig. 5).

Data analysis by nonlinear curve fitting indicated that the K_d increased from 31 nM (control membranes) to 77 nM (NEM-treated membranes), whereas the B_{max} decreased from 4.2 nM (1.1 pmol/10^8 ghosts) to 2.9 nM (0.73 pmol/10^8 ghosts). NEM treatment therefore resulted in a decrease in the B_{max}/K_d ratio (the ratio of bound to free T_3 at limitingly low ligand concentration) from 0.134 to 0.038. The low-affinity sites were not affected by the NEM pretreatment. This experiment was repeated with similar results.

Protection with T_3 and Trp partially restored T_3 binding to the high-affinity sites; the B_{max}/K_d ratio was 0.093 (T_3-protected) and 0.080 (Trp-protected). This strongly suggests that the reactive sulfhydryl group(s) form part of a recognition site on the binding protein that is, at least partly, common to T_3 and Trp.

In the same preparation, T_3 influx into ghosts was also inactivated by pretreatment of erythrocytes with NEM, and T_3 and Trp protected the T_3 transport activity by 80% and 55%, respectively (Fig. 5 inset), as expected from results obtained with intact erythrocytes [10]. Taken together, these results show that the -SH

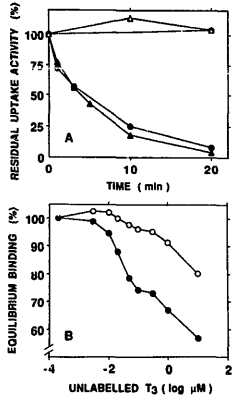

Fig. 6. Effect of phenylglyoxal on T_3 transport, Trp transport, and equilibrium T_3 binding. Rat erythrocytes were preincubated with or without 10 mM phenylglyoxal, washed and incubated overnight as described under Experimental procedures. Panel A: the initial velocities of [^{125}I]T_3 uptake (●, ○) and [^{3}H]Trp uptake (▲, △) were measured (see Experimental procedures) on erythrocytes preincubated for various times with (●, ▲) or without (○, △) phenylglyoxal. Results (mean of duplicates) are expressed as the percentage of zero-time values (0.11 pmol/min per 10^8 cells for T_3 and 19 pmol/min per 10^8 cells for Trp). Panel B: ghosts were prepared from erythrocytes preincubated 20 min with (○) or without (●) phenylglyoxal. Equilibrium T_3 binding was measured and the results (mean of duplicates) were expressed as the percentage of the control value (15 fmol/10^8 ghosts).

group(s) essential for the high-affinity binding and the System T activity have identical properties.

The low-affinity binding of T_3 to human erythrocyte ghosts, shown in Fig. 4B, was not affected by erythrocyte pretreatment with NEM (not shown), although the T_3 transport activity is reported to be NEM-inhibitable [8]. This confirms that the low-affinity binding sites in human erythrocyte ghosts are unrelated to System T functioning.

7. *Effect of phenylglyoxal on the initial velocity of T_3 influx and equilibrium T_3 binding*

Phenylglyoxal interacts irreversibly with arginine residues [24]. Preincubation of rat erythrocytes with phenylglyoxal at 37°C induced a time-dependent, irreversible inactivation of the [^{125}I]T_3 and [^{3}H]Trp transport activities (Fig. 6A). The initial velocity of influx of both substrates was reduced to 5–8% of controls by a 20-min treatment. The T_3 and Trp transport activities were inhibited with identical time-courses, indicating that the arginine residues involved in the both cases had a similar reactivity.

Phenylglyoxal permeates the red cell membrane, reaching arginine residues on both sides of the membrane, but arginine residues that are exposed to an alkaline medium are known to react with phenylglyoxal considerably more rapidly [24]. However, the time-course of inactivation was not modified when the erythrocytes were preincubated at pH 9.1 (not shown), suggesting that the arginine residues involved were located on the intracellular side of the membrane.

Ghosts prepared from phenylglyoxal-treated erythrocytes were studied for equilibrium T_3 binding. Fig. 6B shows that the high-affinity binding was strongly inhibited, whereas the low-affinity sites were not affected. Nonlinear curve fitting gave the following values for control and phenylglyoxal-treated ghosts: K_d = 20 nM, B_{max} = 1.2 pmol/10^8 ghosts (control) and K_d = 64 nM, B_{max} = 0.73 pmol/10^8 ghosts (treated). Alteration of both the apparent affinity and the number of binding sites may indicate the involvement of more than one class of arginine residues. These results again point to a correlation between the inactivation of the T_3/Trp transport system and the inhibition of the high-affinity T_3-binding sites.

Conclusions

The presence of a *trans*-inhibited transport step allows the equilibrium binding in ghosts to be measured after washing with a stop solution. In contrast, the rapid dissociation kinetics requires that binding to inside-out vesicles be measured under strict equilibrium conditions. With these methods, Trp-inhibitable high-affinity T_3 binding sites are detected in rat erythrocyte ghosts and in peripheral protein-depleted vesicles, indicating that they are an integral part of the membrane. The dependence of T_3 binding on -SH groups and arginine residues indicates that the binding sites are, at least partly, of protein nature. Their binding constants and substrate specificity (iodothyronines and amino acids) suggest that they are related to System T. Two additional lines of evidence indicate that they are associated with the carrier. First, cells which have a defective System T lack high-affinity T_3-binding sites. Second, irreversible inhibitors that act on the essential -SH groups and arginine residues have similar effects on T_3 and Trp transport activities and on T_3 binding.

The low-affinity and nonsaturable T_3-binding sites, which were also detected in rat and human erythrocyte ghosts, might be involved in T_3 trapping at the intracellular surface of the erythrocyte membrane. Whether this reflects binding to skeletal proteins, and/or to phospholipids in the inner leaflet of the membrane, remains to be determined.

Transport kinetics [10,13] and binding data (present work) are all compatible with common, or overlapping substrate binding sites for T_3 and Trp that are involved in the transport of both substrates across the rat erythrocyte membrane. The transport kinetics of the two substrates conform to a simple carrier model, which postulates a single substrate binding site per carrier molecule [30]. Therefore, a 1:1 relationship between the number of Trp-inhibitable high-affinity T_3-binding sites and the number of carrier molecules, although not proved unequivocally, seems to be a reasonable assumption. On this basis, the translocation capacity (turnover number) of the carrier may be calculated from the B_{max} for T_3 (present work) and the maximal velocities of zero-*trans* influx in intact erythrocytes [10]. The value for Trp (approx. 220 molecules/site per s at 25°C) is similar to the values (120–190 molecules/site per s at 22°C) reported for the uridine carrier in the erythrocytes of several species [31]. The turnover number for the T_3 transport is more than 100-fold lower (approx. 2 molecules/site per s), due either to slow transconformation, or to slow dissociation of the T_3-carrier complex.

It is not known whether the T_3-specific domain of the substrate binding site of System T is a part of the carrier per se or of a molecule closely associated with the carrier. Comparison of the binding kinetics in ghosts and inside-out vesicles suggests that the high-affinity T_3-binding domain has an intracellular orientation. This does not exclude the existence of an extracellular-oriented, low-affinity conformation involved in T_3 and Trp transport, which could not be characterized with the present methodology. Unequivocal elucidation of the mechanisms of T_3 and aromatic amino acid transport by System T now requires identification and purification of the carrier protein(s) and reconstitution of the transport activities in artificial membranes. High-affinity noncovalent inhibitors of transport, such as cytochalasin B for the glucose carrier [32] or nitrobenzylthioinosine for the nucleoside carrier [33], have been very useful in characterizing transport systems, but specific inhibitors for amino acid transport systems are lacking. T_3 may well be a high-affinity, selective ligand for identifying the components of System T.

References

1 Krenning, E.P., Docter, R., Bernard, H.F., Visser, T.J. and Hennemann, G. (1978) FEBS Lett. 91, 113–116.
2 Holm, A.C., Wong, K.Y., Pliam, N.B., Jorgensen, E.C. and Goldfine, I.D. (1980) Acta Endocrinol. 95, 350–358.
3 Cheng, S.Y. (1983) Endocrinology 112, 1754–1762.
4 Pontecorvi, A. and Robbins, J. (1986) Endocrinology 119, 2755–2761.
5 Blondeau, J.P., Osty, J. and Francon, J. (1988) J. Biol. Chem. 263, 2685–2692.
6 Osty, J., Jego, L., Francon, J. and Blondeau, J.P. (1988) Endocrinology 123, 2303–2311.
7 Osty, J., Zhou, Y., Chantoux, F., Francon, J. and Blondeau, J.P. (1990) Biochim. Biophys. Acta 1051, 46–51.
8 Osty, J., Valensi, P., Samson, M., Francon, J. and Blondeau, J.P. (1990) J. Clin. Endocrinol. Metab. 71, 1589–1595.
9 Francon, J., Osty, J., Chantoux, F. and Blondeau, J.P. (1990) Acta Endocrinol. 122, 341–348.
10 Zhou, Y., Samson, M., Osty, J., Francon, J. and Blondeau, J.P. (1990) J. Biol. Chem. 265, 17000–17004.
11 Rosenberg, R. (1981) Biochim. Biophys. Acta 649, 262–268.
12 Lopez-Burillo, S., Garcia-Sancho, J. and Herreros, B. (1985) Biochim. Biophys. Acta 820, 85–94.
13 Zhou, Y., Samson, M., Francon, J. and Blondeau, J.P. (1992) Biochem. J. 281, 81–86.
14 Pliam, N.B. and Goldfine, I.D. (1977) Biochem. Biophys. Res. Commun. 79, 166–172.
15 Gharbi-Chihi, J. and Torresani, J. (1981) J. Endocrinol. Invest. 4, 177–183.
16 Segal, J. and Ingbar, S.H. (1982) J. Clin. Invest. 70, 919–926.
17 Botta, J.A., De Mendoza, D., Morero, R.D. and Farias, R.N. (1983) J. Biol. Chem. 258, 6690–6692.
18 Segal, J. and Ingbar, S.H. (1980) Endocrinology 107, 1354–1358.
19 De Mendoza, D., Morero, H. and Farias, R.N. (1978) J. Biol. Chem. 253, 6255–6259.
20 Samson, M., Osty, J., Francon, J. and Blondeau, J.P. (1991) Ann. Endocrinol. (Paris) 52, 70.
21 Steck, T.L. and Kant, J.A. (1974) in Methods in Enzymology (Fleischer, S. and Packer, L., eds.), Vol. 31, pp. 172–180, Academic Press, New York.
22 Jarvis, B.J. and Young, J.D. (1981) Biochem. J. 194, 331–339.
23 Bernal, J., Coleoni, A.H. and DeGroot, L.J. (1978) Endocrinology 103, 403–413.
24 Bjerrum, P.J. (1989) in Methods in Enzymology (Fleischer, S. and Fleischer, B., eds.), Vol. 173, pp. 466–494, Academic Press, San Diego, CA.
25 Snedecor, G.W. and Cochran, W.G. (1967) Statistical Methods, 6th Edn., Iowa State University Press, Ames, IA.
26 Munson, P.J. and Rodbard, R. (1980) Anal. Biochem. 107, 220–239.
27 Hopfer, U. (1989) in Methods in Enzymology (Fleischer, S. and Fleischer, B., eds.), Vol. 172, pp. 313–345, Academic Press, San Diego, CA.
28 Devés, R. and Krupka, R.M. (1979) Biochim. Biophys. Acta 556, 533–547.
29 Angel, R.C., Botta, J.A. and Farias, N.R. (1987) Biochim. Biophys. Acta 897, 488–494.
30 Stein, W.D. (1986) in Transport and Diffusion Across Cell Membranes (Stein, W.D., ed.), pp. 231–261, Academic Press, New York.
31 Jarvis, B.J., Hammond, J.R., Paterson, A.R.P. and Clanachan, A.S. (1982) Biochem. J. 208, 83–88.
32 Wheeler, T.J. and Hinkle, P.C. (1985) Annu. Rev. Physiol. 47, 503–517.
33 Plagemann, F.G.W., Wohlhuter, R.M. and Woffendin, C. (1988) Biochim. Biophys. Acta 947, 405–443.